

# New Perspectives on the Structure of Graphitic Carbons

Peter J. F. Harris\*

Centre for Advanced Microscopy, University of Reading, Whiteknights, Reading, RG6 6AF, UK

Graphitic forms of carbon are important in a wide variety of applications, ranging from pollution control to composite materials, yet the structure of these carbons at the molecular level is poorly understood. The discovery of fullerenes and fullerene-related structures such as carbon nanotubes has given a new perspective on the structure of solid carbon. This review aims to show how the new knowledge gained as a result of research on fullerene-related carbons can be applied to well-known forms of carbon such as microporous carbon, glassy carbon, carbon fibers, and carbon black.

**Keywords** fullerenes, carbon nanotubes, carbon nanoparticles, non-graphitizing carbons, microporous carbon, glassy carbon, carbon black, carbon fibers.

## Table of Contents

INTRODUCTION .....	235
FULLERENES, CARBON NANOTUBES, AND CARBON NANOPARTICLES .....	236
MICROPOROUS (NON-GRAPHITIZING) CARBONS .....	239
Background .....	239
Early Models .....	241
Evidence for Fullerene-Like Structures in Microporous Carbons .....	242
New Models for the Structure of Microporous Carbons .....	242
Carbonization and the Structural Evolution of Microporous Carbon .....	243
GLASSY CARBON .....	244
CARBON FIBERS .....	245
CARBON BLACK .....	248
Background .....	248
Structure of Carbon Black Particles .....	249
Effect of High-Temperature Heat Treatment on Carbon Black Structure .....	250
CONCLUSIONS .....	250
ACKNOWLEDGMENTS .....	251
REFERENCES .....	251

## INTRODUCTION

Until quite recently we knew for certain of just two allotropes of carbon: diamond and graphite. The vast range of carbon ma-

terials, both natural and synthetic, which have more disordered structures have traditionally been considered as variants of one or other of these two allotropes. Because the great majority of these materials contain  $sp^2$  carbon rather than  $sp^3$  carbon, their structures have been thought of as being made up from tiny fragments

\*E-mail: p.j.f.harris@rdg.ac.uk

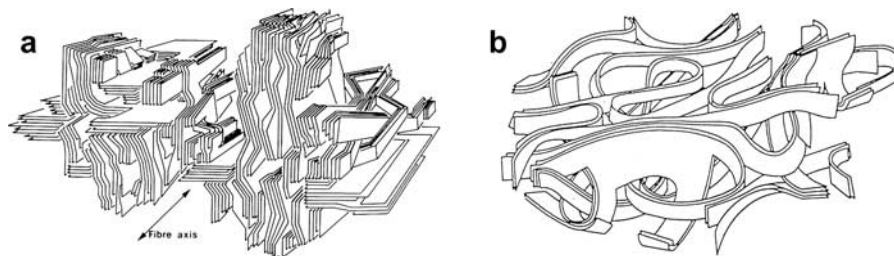


FIG. 1. (a) Model of PAN-derived carbon fibres from the work of Crawford and Johnson,<sup>1</sup> (b) model of a non-graphitizing carbon by Ban and colleagues.<sup>2</sup>

of crystalline graphite. Examples of models for the structures of carbons in which the basic elements are graphitic are reproduced in Figure 1. The structure shown in Figure 1(a) is a model for the structure of carbon fibers suggested by Crawford and Johnson in 1971,<sup>1</sup> whereas 1(b) shows a model for non-graphitizing carbon given by Ban and colleagues in 1975.<sup>2</sup> Both structures are constructed from bent or curved sheets of graphite, containing exclusively hexagonal rings. Although these models probably provide a good first approximation of the structures of these carbons, in many cases they fail to explain fully the properties of the materials. Consider the example of non-graphitizing carbons. As the name suggests, these cannot be transformed into crystalline graphite even at temperatures of 3000°C and above. Instead, high temperature heat treatments transform them into structures with a high degree of porosity but no long-range crystalline order. In the model proposed by Ban *et al.* (Figure 1(b)), the structure is made up of ribbon-like sheets enclosing randomly shaped voids. It is most unlikely that such a structure could retain its porosity when subjected to high temperature heat treatment—surface energy would force the voids to collapse. The shortcomings of this and other “conventional” models are discussed more fully later in the article.

The discovery of the fullerenes<sup>3–5</sup> and subsequently of related structures such as carbon nanotubes,<sup>6–8</sup> nanohorns,<sup>9,10</sup> and nanoparticles,<sup>11</sup> has given us a new paradigm for solid carbon structures. We now know that carbons containing pentagonal rings, as well as other non-six-membered rings, among the hexagonal  $sp^2$  carbon network, can be highly stable. This new perspective has prompted a number of groups to take a fresh look at well-known forms of carbon, to see whether any evidence can be found for the presence of fullerene-like structures.<sup>12–14</sup> The aim of this article is to review this new work on the structure of graphitic carbons, to assess whether models that incorporate fullerene-like elements could provide a better basis for understanding these materials than the conventional models, and to point out areas where further work is needed. The carbon materials considered include non-graphitizing carbon, glassy carbon, carbon fibers, and carbon black. The article begins with an outline of the main structural features of fullerenes, carbon nanotubes, and carbon nanoparticles, together with a brief discussion of their stability.

### FULLERENES, CARBON NANOTUBES, AND CARBON NANOPARTICLES

The structure of  $C_{60}$ , the archetypal fullerene, is shown in Figure 2(a). The structure consists of twelve pentagonal rings and twenty hexagons in an icosahedral arrangement. It will be noted that all the pentagons are isolated from each other. This is important, because adjacent pentagonal rings form an unstable bonding arrangement. All other closed-cage isomers of  $C_{60}$ , and all smaller fullerenes, are less stable than buckminsterfullerene because they have adjacent pentagons. For higher fullerenes, the number of structures with isolated pentagonal rings increases rapidly with size. For example,  $C_{100}$  has 450 isolated-pentagon isomers.<sup>16</sup> Most of these higher fullerenes have low symmetry; only a very small number of them have the icosahedral symmetry of  $C_{60}$ . An example of a giant fullerene that can have icosahedral symmetry is  $C_{540}$ , as shown in Figure 2(b).

There have been many studies of the stability of fullerenes as a function of size (e.g., Refs. 17, 18). These show that, in general, stability increases with size. Experimentally, there is evidence that  $C_{60}$  is unstable with respect to large, multiwalled fullerenes. This was demonstrated by Mochida and colleagues, who heated  $C_{60}$  and  $C_{70}$  in a sublimation-limiting furnace.<sup>19</sup> They showed that the cage structure broke down at 900°C–1000°C, although at 2400°C fullerene-like “hollow spheres” with diameters in the range 10–20 nm were formed.

We now consider fullerene-related carbon nanotubes, which were discovered by Iijima in 1991.<sup>6</sup> These consist of cylinders of graphite, closed at each end with caps that contain precisely six pentagonal rings. We can illustrate their structure by considering the two “archetypal” carbon nanotubes that can be formed by cutting a  $C_{60}$  molecule in half and placing a graphene cylinder between the two halves. Dividing  $C_{60}$  parallel to one of the threefold axes results in the zig-zag nanotube shown in Figure 3(a), whereas bisecting  $C_{60}$  along one of the fivefold axes produces the armchair nanotube shown in Figure 3(b). The terms “zig-zag” and “armchair” refer to the arrangement of hexagons around the circumference. There is a third class of structure in which the hexagons are arranged helically around the tube axis. Experimentally, the tubes are generally much less perfect than the idealized versions shown in Figure 3, and may be either

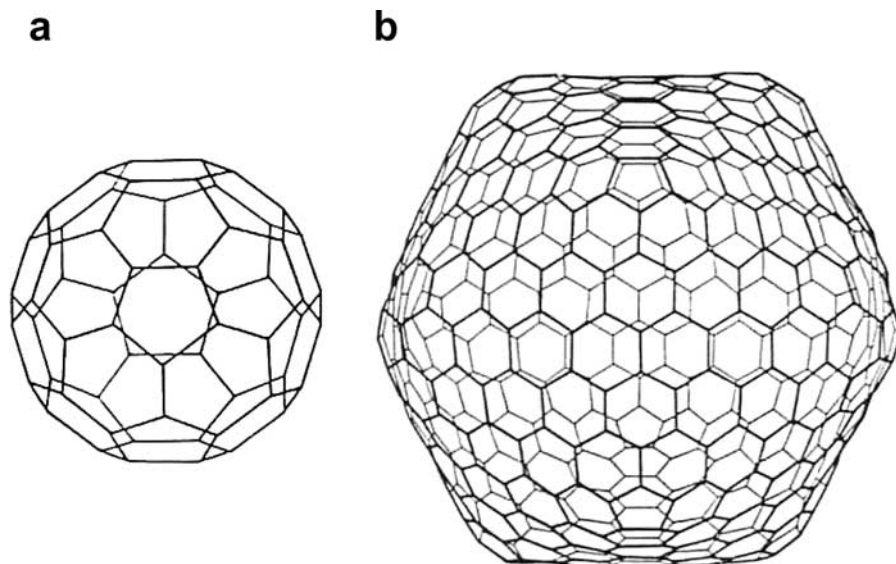


FIG. 2. The structure of (a)  $C_{60}$ , (b) icosahedral  $C_{540}$ .<sup>15</sup>

multilayered or single-layered. Figure 4 shows a high resolution TEM image of multilayered nanotubes. The multilayered tubes range in length from a few tens of nm to several microns, and in outer diameter from about 2.5 nm to 30 nm. The end-caps of the tubes are sometimes symmetrical in shape, but more often asymmetric. Conical structures of the kind shown in Figure 5(a) are commonly observed. This type of structure is believed to result from the presence of a single pentagon at the position indicated by the arrow, with five further pentagons at the apex of the cone. Also quite common are complex cap structures displaying a “bill-like” morphology such as that shown

in Figure 5(b).<sup>21</sup> This structure results from the presence of a single pentagon at point “X” and a heptagon at point “Y.” The heptagon results in a saddle-point, or region of negative curvature.

The nanotubes first reported by Iijima were prepared by vaporizing graphite in a carbon arc under an atmosphere of helium. Nanotubes produced in this way are invariably accompanied by other material, notably carbon nanoparticles. These can be thought of as giant, multilayered fullerenes, and range in size from  $\sim 5$  nm to  $\sim 15$  nm. A high-resolution image of a nanoparticle attached to a nanotube is shown in Figure 6(a).<sup>22</sup> In this

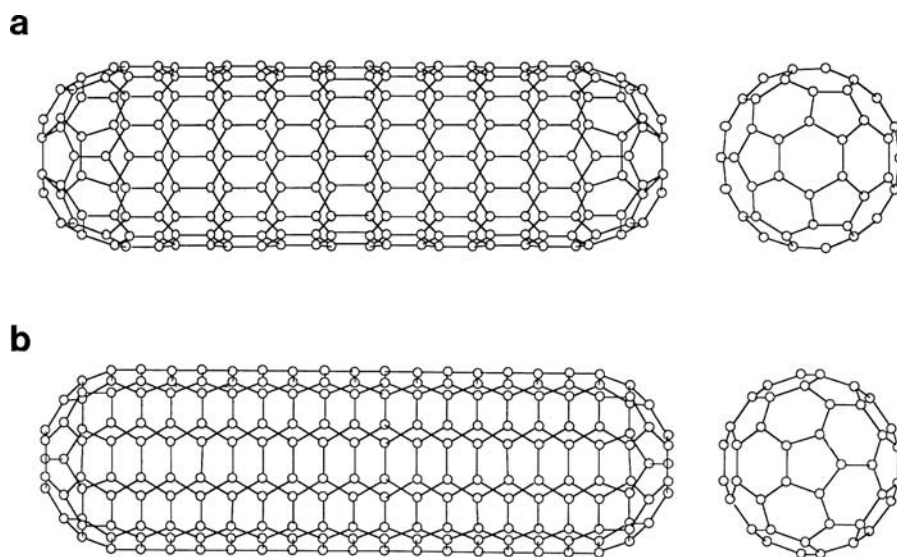


FIG. 3. Drawings of the two nanotubes that can be capped by one half of a  $C_{60}$  molecule. (a) Zig-zag (9, 0) structure, (b) armchair (5, 5) structure.<sup>20</sup>

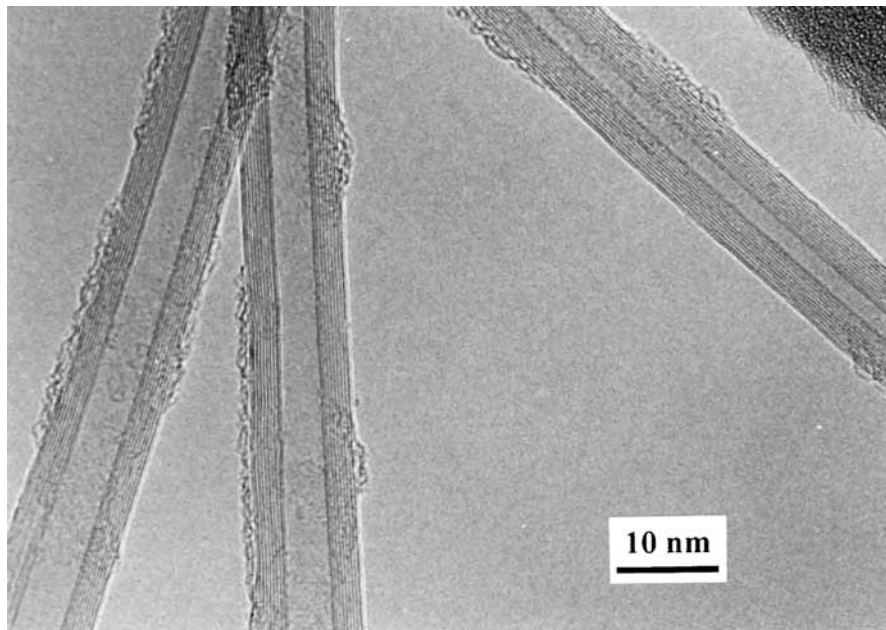


FIG. 4. TEM image of multiwalled nanotubes.

case, the particle consists of three concentric fullerene shells. A more typical nanoparticle, with many more layers, is shown in Figure 6(b). These larger particles are probably relatively imperfect in structure.

Single-walled nanotubes were first prepared in 1993 using a variant of the arc-evaporation technique.<sup>23,24</sup> These are quite different from multilayered nanotubes in that they generally have very small diameters (typically  $\sim 1$  nm), and tend to be curled

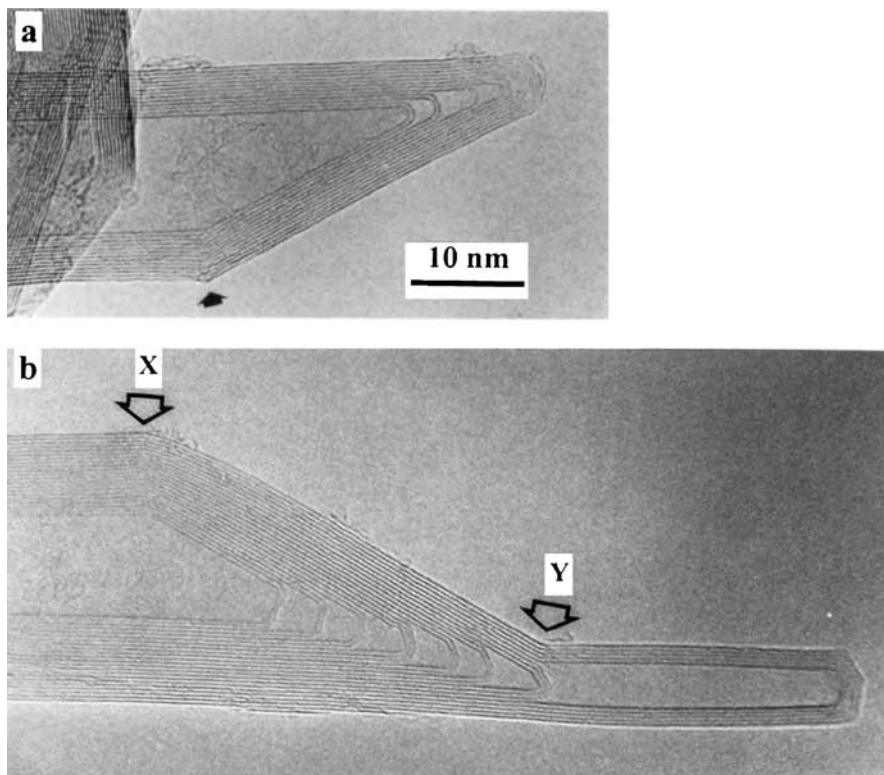


FIG. 5. Images of typical multiwalled nanotube caps. (a) cap with asymmetric cone structure, (b) cap with bill-like structure.<sup>21</sup>

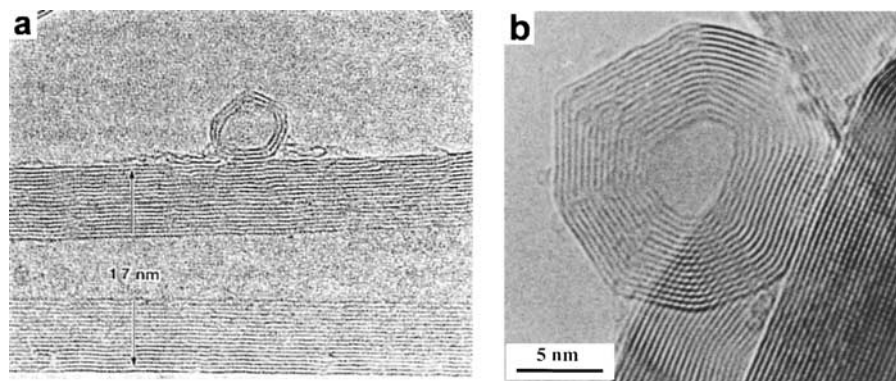


FIG. 6. Images of carbon nanoparticles. (a) small nanoparticle with three concentric layers on nanotube surface,<sup>22</sup> (b) larger multilayered nanoparticle.

and looped rather than straight. They will not be considered further here because they have no parallel among well-known forms of carbon discussed in this article.

The stability of multilayered carbon nanotubes and nanoparticles has not been studied in detail experimentally. However, we know that they are formed at the center of graphite electrodes during arcing, where temperatures probably approach 3000°C. It is reasonable to assume, therefore, that nanotubes and nanoparticles could withstand being re-heated to such temperatures (in an inert atmosphere) without significant change.

### MICROPOROUS (NON-GRAPHITIZING) CARBONS

#### Background

It was demonstrated many years ago by Franklin<sup>25,26</sup> that carbons produced by the solid-phase pyrolysis of organic materials fall into two distinct classes. The so-called graphitizing carbons tend to be soft and non-porous, with relatively high densities, and can be readily transformed into crystalline graphite by heating at temperatures in the range 2200°C–3000°C. In contrast, “non-graphitizing” carbons are hard, low-density materi-

als that cannot be transformed into crystalline graphite even at temperatures of 3000°C and above. The low density of non-graphitizing carbons is a consequence of a microporous structure, which gives these materials an exceptionally high internal surface area. This high surface area can be enhanced further by activation, that is, mild oxidation with a gas or chemical processing, and the resulting “activated carbons” are of enormous commercial importance, primarily as adsorbents.<sup>27–29</sup>

The distinction between graphitizing and non-graphitizing carbons can be illustrated most clearly using transmission electron microscopy (TEM). Figure 7(a) shows a TEM image of a typical non-graphitizing carbon prepared by the pyrolysis of sucrose in an inert atmosphere at 1000°C.<sup>30</sup> The inset shows a diffraction pattern recorded from an area approximately 0.25  $\mu\text{m}$  in diameter. The image shows the structure to be disordered and isotropic, consisting of tightly curled single carbon layers, with no obvious graphitization. The diffraction pattern shows symmetrical rings, confirming the isotropic structure. The appearance of graphitizing carbons, on the other hand, approximates much more closely to that of graphite. This can be seen in the TEM micrograph of a carbon prepared from anthracene,

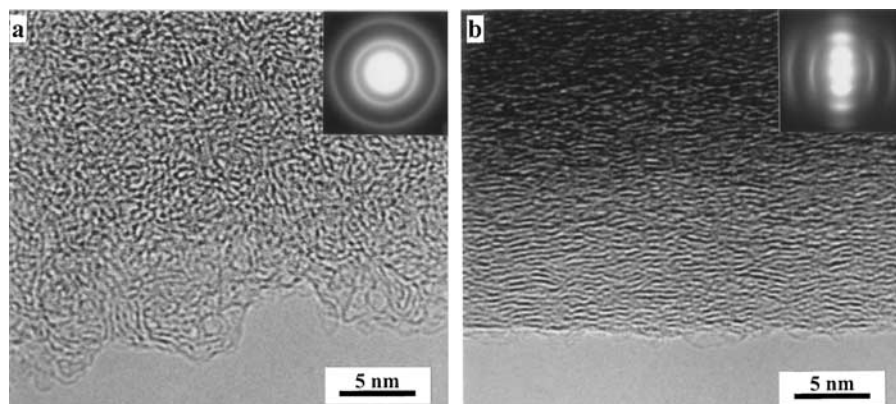


FIG. 7. (a) High resolution TEM image of carbon prepared by pyrolysis of sucrose in nitrogen at 1000°C, (b) carbon prepared by pyrolysis of anthracene at 1000°C. Insets show selected area diffraction patterns.<sup>30</sup>

which is shown in Figure 7(b). Here, the structure contains small, approximately flat carbon layers, packed tightly together with a high degree of alignment. The fragments can be considered as rather imperfect graphene sheets. The diffraction pattern for the graphitizing carbon consists of arcs rather than symmetrical rings, confirming that the layers are preferentially aligned along a particular direction. The bright, narrow arcs in this pattern correspond to the interlayer  $\{0002\}$  spacings, whereas the other reflections appear as broader, less intense arcs.

Transmission electron micrographs showing the effect of high-temperature heat treatments on the structure of non-graphitizing and graphitizing carbons are shown in Figure 8 (note that the magnification here is much lower than for Figure 7). In the case of the non-graphitizing carbon, heating at 2300°C in an inert atmosphere produces the disordered, porous material shown in Figure 8(a). This structure is made up of curved and faceted graphitic layer planes, typically 1–2 nm thick and 5–15 nm in length, enclosing randomly shaped pores. A few somewhat larger graphite crystallites are present, but there is no macroscopic graphitization. In contrast, heat treatment of the anthracene-derived carbon produces large crystals of highly ordered graphite, as shown in Figure 8(b).

Other physical measurements also demonstrate sharp differences between graphitizing and non-graphitizing carbons. Table 1 shows the effect of preparation temperature on the surface areas and densities of a typical graphitizing carbon prepared from polyvinyl chloride, and a non-graphitizing carbon prepared from cellulose.<sup>31</sup> It can be seen that the graphitizing carbon prepared at 700°C has a very low surface area, which changes little for carbons prepared at higher temperatures, up to 3000°C. The density of the carbons increases steadily as the preparation

TABLE 1  
Effect of temperature on surface areas and densities of carbons prepared from polyvinyl chloride and cellulose<sup>31</sup>

(a) Surface areas

Starting material	Specific surface area (m <sup>2</sup> /g) for carbons prepared at:				
	700°C	1500°C	2000°C	2700°C	3000°C
PVC	0.58	0.21	0.21	0.71	0.56
Cellulose	408	1.60	1.17	2.23	2.25

(b) Densities

Starting material	Helium density (g/cm <sup>3</sup> ) for carbons prepared at:				
	700°C	1500°C	2000°C	2700°C	3000°C
PVC	1.85	2.09	2.14	2.21	2.26
Cellulose	1.90	1.47	1.43	1.56	1.70

temperature is increased, reaching a value of 2.26 g/cm<sup>3</sup>, which is the density of pure graphite, at 3000°C. The effect of preparation temperature on the non-graphitizing carbon is very different. A high surface area is observed for the carbon prepared at 700°C (408 m<sup>2</sup>/g), which falls rapidly as the preparation temperature is increased. Despite this reduction in surface area, however, the density of the non-graphitizing carbon actually falls when the temperature of preparation is increased. This indicates that a high proportion of “closed porosity” is present in the heat-treated carbon.

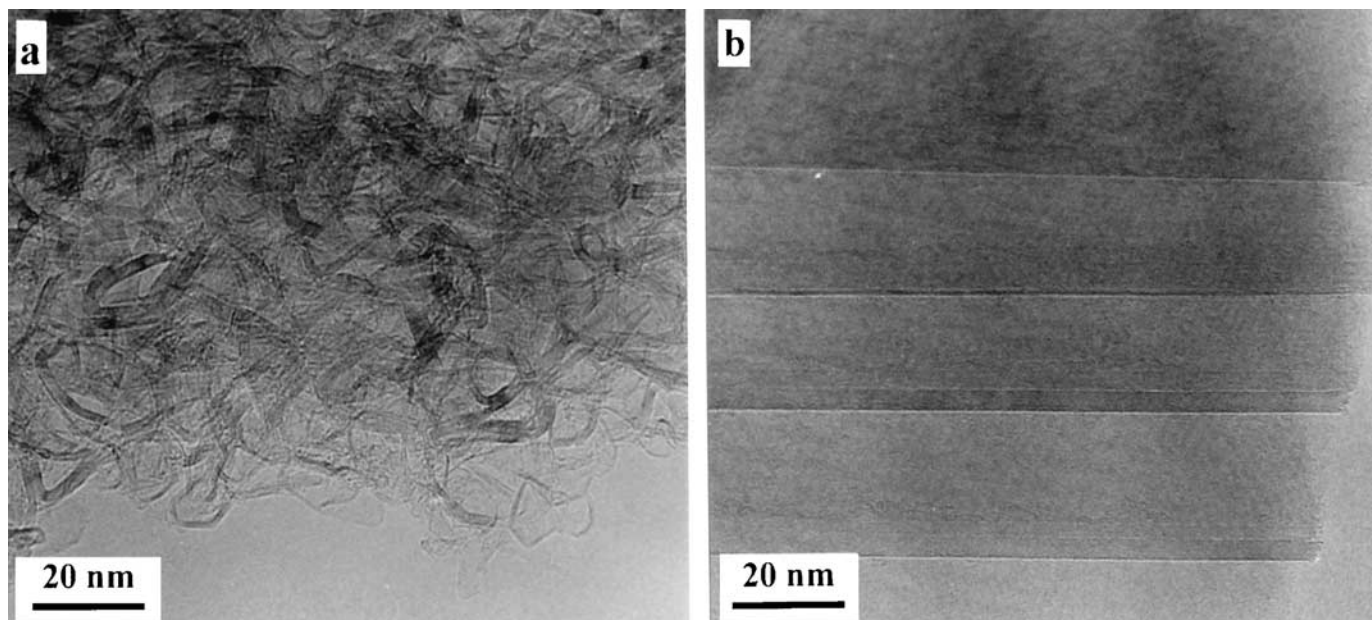


FIG. 8. Micrographs of (a) sucrose carbon and (b) anthracene carbon following heat treatment at 2300°C.

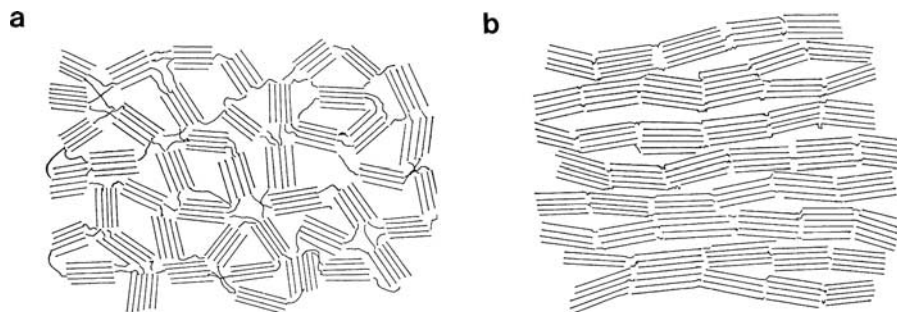


FIG. 9. Franklin's representations of (a) non-graphitizing and (b) graphitizing carbons.<sup>25</sup>

### Early Models

The first attempt to develop structural models of graphitizing and non-graphitizing carbons was made by Franklin in her 1951 paper.<sup>25</sup> In these models, the basic units are small graphitic crystallites containing a few layer planes, which are joined together by crosslinks. The precise nature of the crosslinks is not specified. An illustration of Franklin's models is shown in Figure 9. Using these models, she put forward an explanation of why non-graphitizing carbons cannot be converted by heat treatment into graphite, and this will now be summarized. During carbonization the incipient stacking of the graphene sheets in the non-graphitizing carbon is largely prevented. At this stage the presence of crosslinks, internal hydrogen, and the viscosity of the material is crucial. The resulting structure of the carbon (at  $\sim 1000^\circ\text{C}$ ) consists of randomly ordered crystallites, held together by residual crosslinks and van der Waals forces, as in Figure 9(a). During high-temperature treatment, even though these crosslinks may be broken, the activation energy for the motion of entire crystallites, required for achieving the structure of graphite, is too high and graphite is not formed. On the other hand, the structural units in a graphitizing carbon are approximately parallel to each other, as in Figure 9(b), and the transformation of such a structure into crystalline graphite would be expected to be relatively facile. Although Franklin's ideas on graphitizing and non-graphitizing carbons may be broadly correct, they are in some regards incomplete. For example, the nature of the crosslinks between the graphitic fragments is not specified, so the reasons for the sharply differing properties of graphitizing and non-graphitizing carbons is not explained.

The advent of high-resolution transmission electron microscopy in the early 1970s enabled the structure of non-graphitizing carbons to be imaged directly. In a typical study, Ban, Crawford, and Marsh<sup>2</sup> examined carbons prepared from polyvinylidene chloride (PVDC) following heat treatments at temperatures in the range  $530^\circ\text{C}$ – $2700^\circ\text{C}$ . Images of these carbons apparently showed the presence of curved and twisted graphite sheets, typically two or three layer planes thick, enclosing voids. These images led Ban *et al.* to suggest that heat-treated non-graphitizing carbons have a ribbon-like structure, as shown in Figure 1(b). This structure corresponds to a PVDC carbon heat treated at  $1950^\circ\text{C}$ . This ribbon-like model is rather similar

to an earlier model of glassy carbon proposed by Jenkins and Kawamura.<sup>32</sup> However, models of this kind, which are intended to represent the structure of non-graphitizing carbons following high-temperature heat treatment, have serious weaknesses, as noted earlier. Such models consist of curved and twisted graphene sheets enclosing irregularly shaped pores. However, graphene sheets are known to be highly flexible, and would therefore be expected to become ever more closely folded together at high temperatures, in order to reduce surface energy. Indeed, tightly folded graphene sheets are quite frequently seen in carbons that have been exposed to extreme conditions.<sup>33</sup> Thus, structures like the one shown in Figure 1(b) would be unlikely to be stable at very high temperatures.

It has also been pointed out by Oberlin<sup>34,35</sup> that the models put forward by Jenkins, Ban, and their colleagues were based on a questionable interpretation of the electron micrographs. In most micrographs of partially graphitized carbons, only the  $\{0002\}$  fringes are resolved, and these are only visible when they are approximately parallel to the electron beam. Therefore, such images tend to have a ribbon-like appearance. However, because only a part of the structure is being imaged, this appearance can be misleading, and the true three-dimensional structure may be more cagelike than ribbon-like. This is a very important point, and must always be borne in mind when analyzing images of graphitic carbons. Oberlin herself believes that all graphitic carbons are built up from basic structural units, which comprise small groups of planar aromatic structures,<sup>35</sup> but does not appear to have given a detailed explanation for the non-graphitizability of certain carbons.

The models of non-graphitizing carbons described so far have assumed that the carbon atoms are exclusively  $sp^2$  and are bonded in hexagonal rings. Some authors have suggested that  $sp^3$ -bonded atoms may be present in these carbons (e.g., Refs. 36, 37), basing their arguments on an analysis of X-ray diffraction patterns. The presence of diamond-like domains would be consistent with the hardness of non-graphitizing carbons, and might also explain their extreme resistance to graphitization. A serious problem with these models is that  $sp^3$  carbon is unstable at high temperatures. Diamond is converted to graphite at  $1700^\circ\text{C}$ , whereas tetrahedrally bonded carbon atoms in amorphous films are unstable above about  $700^\circ\text{C}$ . Therefore, the

presence of  $sp^3$  atoms in a carbon cannot explain the resistance of the carbon to graphitization at high temperatures. It should also be noted that more recent diffraction studies of non-graphitizing carbons have suggested that  $sp^3$ -bonded atoms are not present, as discussed further in what follows.

### Evidence for Fullerene-Like Structures in Microporous Carbons

The evidence that microporous carbons might have fullerene-related structures has come mainly from high-resolution TEM studies. The present author and colleagues initiated a series of studies of typical non-graphitizing microporous carbons using this technique in the mid 1990s.<sup>30,38,39</sup> The first such study involved examining carbons prepared from PVDC and sucrose, after heat treatments at temperatures in the range 2100°C–2600°C.<sup>38</sup> The carbons subjected to very high temperatures had rather disordered structures similar to that shown in Figure 8(a). Careful examination of the heated carbons showed that they often contained closed nanoparticles; examples can be seen in Figure 10. The particles were usually faceted, and often hexagonal or pentagonal in shape. Sometimes, faceted layer planes enclosed two or more of the nanoparticles, as shown in Figure 10(b). Here, the arrows indicate two saddle-points, similar to that shown in Figure 5(b). The closed nature of the nanoparticles, their hexagonal or pentagonal shapes, and other features such as the saddle-points strongly suggest that the particles have fullerene-like structures. Indeed, in many cases the particles resemble those produced by arc-evaporation in a fullerene generator (see Figure 6) although in the latter case the particles usually contain many more layers.

The observation of fullerene-related nanoparticles in the heat treated carbons suggested that the original, freshly prepared carbons may also have had fullerene-related structures (see next section). However, obtaining direct evidence for this is difficult. High resolution electron micrographs of freshly prepared carbons, such as that shown in Figure 7(a), are usually rather

featureless, and do not reveal the detailed structure. Occasionally, however, very small closed particles can be found in the carbons.<sup>30</sup> The presence of such particles provides circumstantial evidence that the surrounding carbon may have a fullerene-related structure. Direct imaging of pentagonal rings by HRTEM has not yet been achieved, but recent developments in TEM imaging techniques suggest that this may soon be possible, as discussed in the Conclusions.

As well as high-resolution TEM, diffraction methods have been widely applied to microporous and activated carbons (e.g., Refs. 40–44). However, the interpretation of diffraction data from these highly disordered materials is not straightforward. As already mentioned, some early X-ray diffraction studies were interpreted as providing evidence for the presence of  $sp^3$ -bonded atoms. More recent neutron diffraction studies have suggested that non-graphitizing carbons consist entirely of  $sp^2$  atoms.<sup>40</sup> It is less clear whether diffraction methods can establish whether the atoms are bonded in pentagonal or hexagonal rings. Both Petkov *et al.*<sup>42</sup> and Zetterstrom and colleagues<sup>43</sup> have interpreted neutron diffraction data from nanoporous carbons in terms of a structure containing non-hexagonal rings, but other interpretations may also be possible.

Raman spectroscopy is another valuable technique for the study of carbons.<sup>45</sup> Burian and Dore have used this method to analyze carbons prepared from sucrose, heat treated at temperatures from 1000°C–2300°C.<sup>46</sup> The Raman spectra showed clear evidence for the presence of fullerene- and nanotube-like elements in the carbons. There was also some evidence for fullerene-like structures in graphitizing carbons prepared from anthracene, but these formed at higher temperatures and in much lower proportions than in the non-graphitizing carbons.

### New Models for the Structure of Microporous Carbons

Prompted by the observations described in the previous section, the present author and colleagues proposed a model for the structure of non-graphitizing carbons that consists of

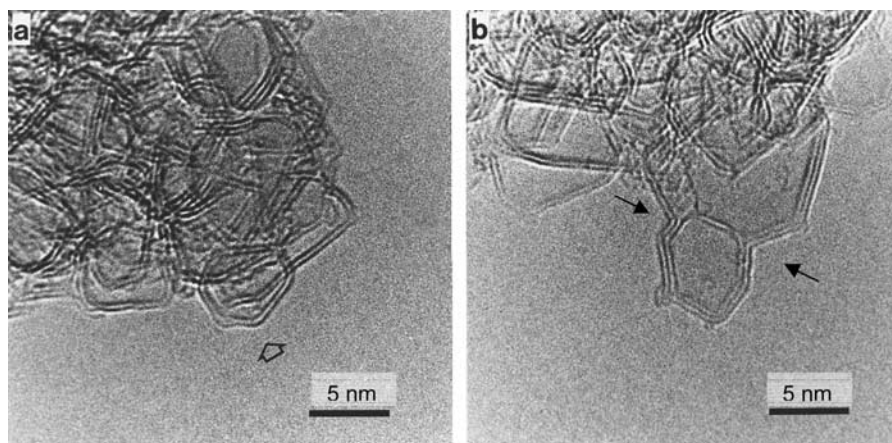


FIG. 10. (a) Micrograph showing closed structure in PVDC-derived carbon heated at 2600°C, (b) another micrograph of same sample, with arrows showing regions of negative curvature.<sup>38</sup>

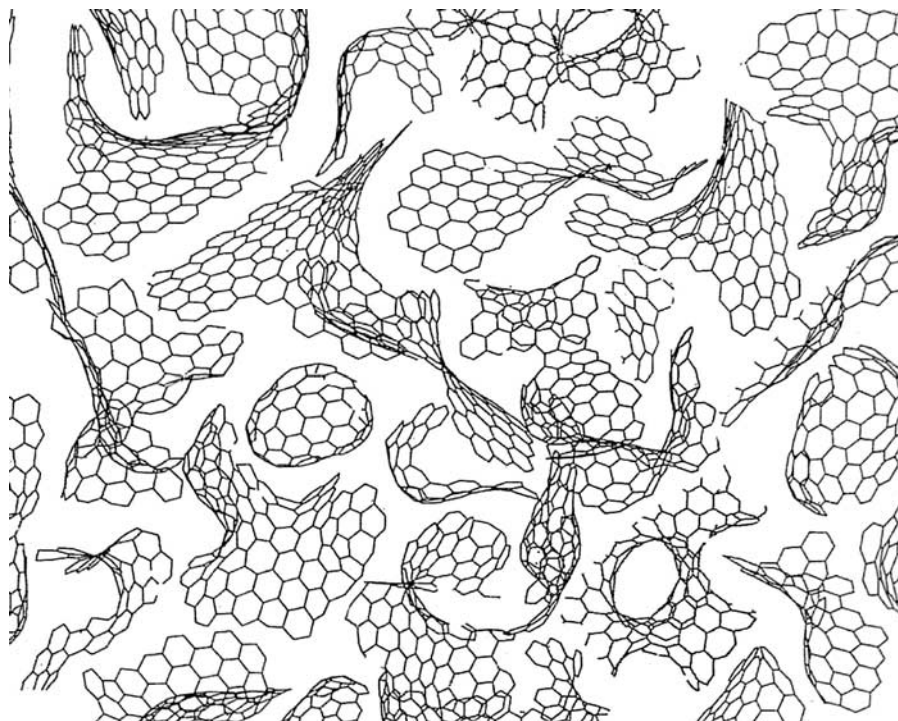


FIG. 11. Schematic illustration of a model for the structure of non-graphitizing carbons based on fullerene-like elements.

discrete fragments of curved carbon sheets, in which pentagons and heptagons are dispersed randomly throughout networks of hexagons, as illustrated in Figure 11.<sup>38,39</sup> The size of the micropores in this model would be of the order of 0.5–1.0 nm, which is similar to the pore sizes observed in typical microporous carbons. The structure has some similarities to the “random schwarzite” network put forward by Townsend and colleagues in 1992,<sup>47</sup> although this was not proposed as a model for non-graphitizing carbons. If the model we have proposed for non-graphitizing carbons is correct it suggests that these carbons are very similar in structure to fullerene soot, the low-density, disordered material that forms on walls of the arc-evaporation vessel and from which  $C_{60}$  and other fullerenes may be extracted. Fullerene soot is known to be microporous, with a surface area, after activation with carbon dioxide, of approximately  $700 \text{ m}^2 \text{ g}^{-1}$ ,<sup>48</sup> and detailed analysis of high resolution TEM micrographs of fullerene soot has shown that these are consistent with a structure in which pentagons and heptagons are distributed randomly throughout a network of hexagons.<sup>49,50</sup> It is significant that high-temperature heat treatments can transform fullerene soot into nanoparticles very similar to those observed in heated microporous carbon.<sup>51,52</sup>

### Carbonization and the Structural Evolution of Microporous Carbon

The process whereby organic materials are transformed into carbon by heat treatment is not well understood at the atomic level.<sup>53,54</sup> In particular, the very basic question of why some

organic materials produce graphitizing carbons and others yield non-graphitizing carbons has not been satisfactorily answered. It is known, however, that both the chemistry and physical properties of the precursors are important in determining the class of carbon formed. Thus, non-graphitizing carbons are formed, in general, from substances containing less hydrogen and more oxygen than graphitizing carbons. As far as physical properties are concerned, materials that yield graphitizing carbons usually form a liquid on heating to temperatures around  $400^\circ\text{C}$ – $500^\circ\text{C}$ , whereas those that yield non-graphitizing carbons generally form solid chars without melting. The liquid phase produced on heating graphitizing carbons is believed to provide the mobility necessary to form oriented regions. However, this may not be a complete explanation, because some precursors form non-graphitizing carbons despite passing through a liquid phase.

The idea that non-graphitizing carbons contain pentagons and other non-six-membered rings, whereas graphitizing carbons consist entirely of hexagonal rings may help in understanding more fully the mechanism of carbonization. Recently Kumar *et al.* have used Monte Carlo (MC) simulations to model the evolution of a polymer structure into a microporous carbon structure containing non-hexagonal rings.<sup>55</sup> They chose polyfurfuryl alcohol, a well-known precursor for non-graphitizing carbon, as the starting material. The polymer was represented as a cubic lattice decorated with the repeat units, as shown in Figure 12(a). All the non-carbon atoms (i.e., hydrogen and oxygen) were then removed from the polymer and this network was used in the

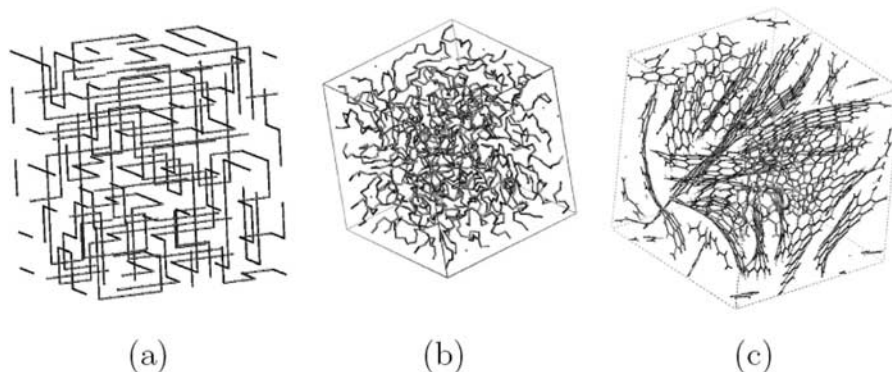


FIG. 12. Monte Carlo simulation showing evolution of amorphous polymer backbone into a linear carbon polymer and then into a disordered  $sp^2$  carbon structure.<sup>55</sup>

MC simulations as the starting structure. An example of such a starting structure folded inside a cubic periodic box is shown in Figure 12(b). The final structure obtained after 4000 MC cycles at  $T = 800^\circ\text{C}$ , with a pre-defined density of  $1.72\text{ g/cm}^3$ , is shown in Figure 12(c). Simulations were carried out with a number of different polymer starting structures and different pre-defined densities. In each case the final carbon was made up of a hexagonal network with 10–15% non-hexagonal rings (pentagons and heptagons). The properties of the simulated carbons appeared to be generally consistent with experimental results.

Acharya *et al.* have used a slightly different approach to model the structural evolution of a microporous carbon.<sup>56</sup> Like Kumar *et al.* they assumed the carbon to be derived from polyfurfuryl alcohol, but started the simulation with a series of all-hexagon fragments, terminated with hydrogens, rather than with the polymer itself. The starting structure is shown in Figure 13(a), whereas Figure 13(b)–(d) illustrate the evolution of the structure as the H/C ratio is reduced (i.e., the temperature is increased). During this evolution, pentagons and heptagons form as well as hexagons. It would be of great interest to extend such simulations to polymers that yield graphitizing rather than non-graphitizing carbons.

### GLASSY CARBON

Glassy carbon is a class of non-graphitizing carbon that is widely used as an electrode material in electrochemistry and for high-temperature crucibles. It is prepared by subjecting the organic precursors to a series of heat treatments at temperatures up to  $3000^\circ\text{C}$ .<sup>57–59</sup> Unlike many non-graphitizing carbons, it is impermeable to gases and chemically extremely inert, especially when prepared at very high temperatures. It has been demonstrated that the rates of oxidation of glassy carbon in oxygen, carbon dioxide, or water vapor are lower than those of any other carbon.<sup>59</sup> It is also highly resistant to attack by acids. Thus, whereas normal graphite is reduced to a powder by a mixture of concentrated sulphuric and nitric acids at room temperature, glassy carbon is unaffected by such treatment, even after several months.

Figure 14, taken from a recent study by the present author,<sup>60</sup> shows HRTEM micrographs of two commercial glassy carbons. Both were prepared from crosslinked aromatic polymers. The carbon shown in Figure 14(a) was prepared at a temperature of  $1000^\circ\text{C}$ , and has a highly disordered, microporous structure made up of tightly curled graphene layers, very similar to that of the non-graphitizing carbon shown in Figure 7(a). The carbon shown in Figure 14(b) was prepared at a temperature of approximately  $3000^\circ\text{C}$ , and has larger pores bounded by faceted or curved single- or multilayered graphitic fragments.

The structure of glassy carbon has been the subject of research since it was first produced in the early 1960s. Some of the earliest structural models assumed that both  $sp^2$  and  $sp^3$ -bonded atoms were present (e.g., Ref. 61). Graphitic domains were envisaged to be interspersed with tetrahedral domains, perhaps linked by short oxygen-containing bridges. These models were based primarily on an analysis of X-ray diffraction measurements and such measurements can be open to a number of interpretations. It should be noted that neutron diffraction data has shown a complete absence of tetrahedrally bonded domains in glassy carbon heat treated at  $2000^\circ\text{C}$ .<sup>62</sup> A different model for the structure of glassy carbon was put forward by Jenkins and colleagues.<sup>32,58,59</sup> This model, illustrated in Figure 15, is based on the assumption that the molecular orientation of the polymeric precursor material is memorized to some extent after carbonization. Thus, the structure bears some resemblance to that of a polymer, in which the “fibrils” are very narrow curved and twisted ribbons of graphitic carbon. The Jenkins–Kawamura model has been quite widely accepted, but appears to be deficient in a number of aspects. For example, a structure such as that shown in Figure 15, with many conjoined micropores, would be expected to be permeable to gases, whereas we know that glassy carbons are highly impermeable. The structure also has a high proportion of edge atoms, which are known to have a relatively high reactivity compared with “in-plane” carbon atoms. This is inconsistent with the known low reactivity of glassy carbon, mentioned earlier. Russian workers have recently proposed a model for glassy carbon that incorporates carbyne-like

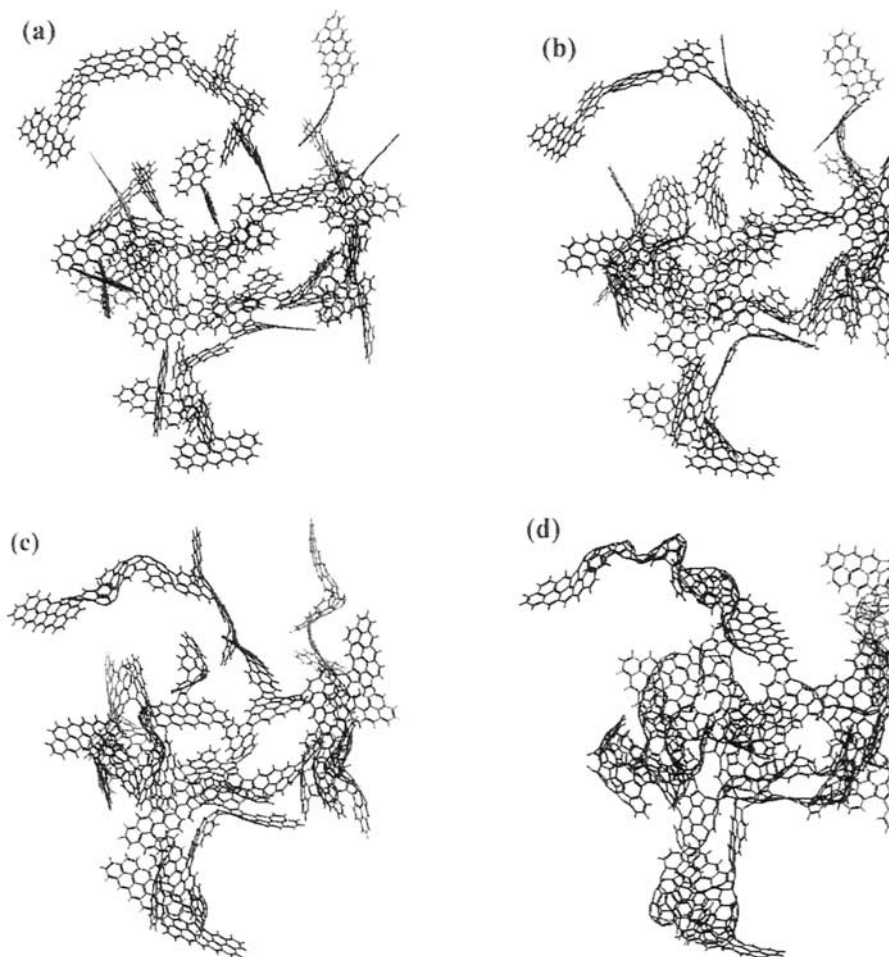


FIG. 13. Simulation of structural evolution of a carbon nanostructure as a function of decreasing H/C ratio or increasing temperature.<sup>56</sup>

chains.<sup>63,64</sup> This model was based partly on a consideration of the electronic properties of glassy carbon but, as the authors themselves accept, there is no direct experimental support for their structure.

Detailed HRTEM studies of the two commercial glassy carbons shown in Figure 14 have revealed the presence of many apparently fullerene-like elements.<sup>60</sup> The presence of such structures strongly suggests that glassy carbons, like other non-graphitizing carbons, may have fullerene-related microstructures. It seems likely that the low temperature glassy carbons may have structures similar to that shown in Figure 11, but perhaps with a higher proportion of completely closed particles, or a more tightly packed microstructure. This would be consistent with the low reactivity of glassy carbon compared with other non-graphitizing carbons. A model for the structure of high temperature glassy carbon is shown in Figure 16. This can be thought of as mainly consisting of broken or imperfect fullerene-related nanoparticles, most of which are multi-layered, enclosing pores that are much larger than in the low-temperature glassy carbons. The presence of seven-membered

rings produces some saddle-points in the structure. A few completely closed nanoparticles will also be present. Fullerene-related models for glassy carbons appear to have significant advantages over earlier ideas about the structure of these carbons, such as those put forward by Jenkins and Kawamura. The fullerene-related models provide a more realistic explanation for the low reactivity, hardness, and impermeability of glassy carbons.

Finally in this section, it is worth mentioning an interesting study by Gogotsi *et al.*<sup>65</sup> These workers have shown that commercial glassy carbon can contain polyhedral graphite crystals, some of which resemble giant nanotubes. The presence of such crystals in glassy carbon is a further indication that it may have a fullerene-like structure.

### CARBON FIBERS

Carbon fibers are used in a host of applications, ranging from aircraft to sporting equipment.<sup>66</sup> They are produced by the pyrolysis of organic precursors, the most common of which are polyacrylonitrile (PAN) and mesophase pitch.<sup>67-70</sup> The

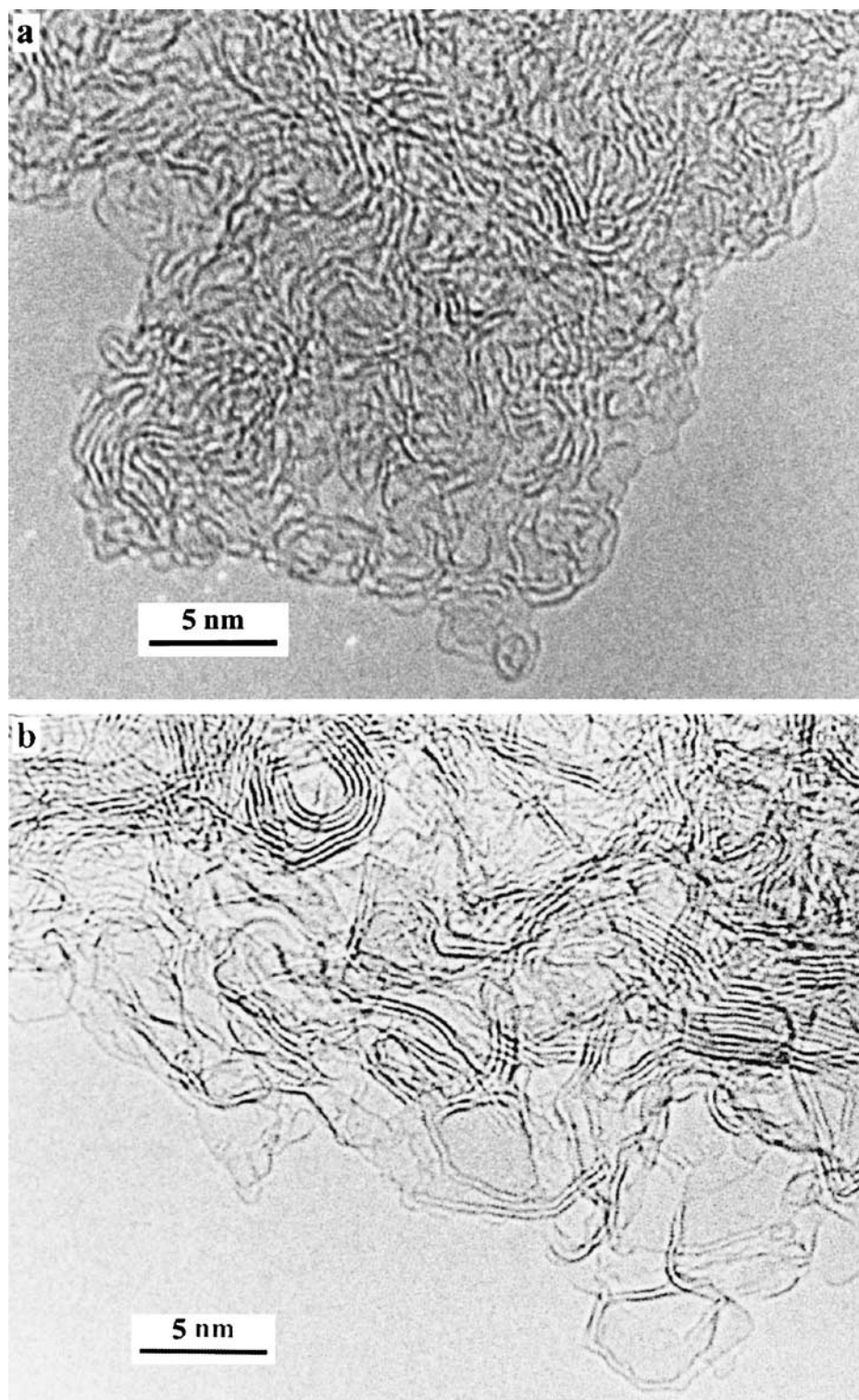


FIG. 14. (a) HRTEM image of commercial glassy carbon prepared at 1000°C (b) image of glassy carbon, prepared at 3000°C.<sup>60</sup>

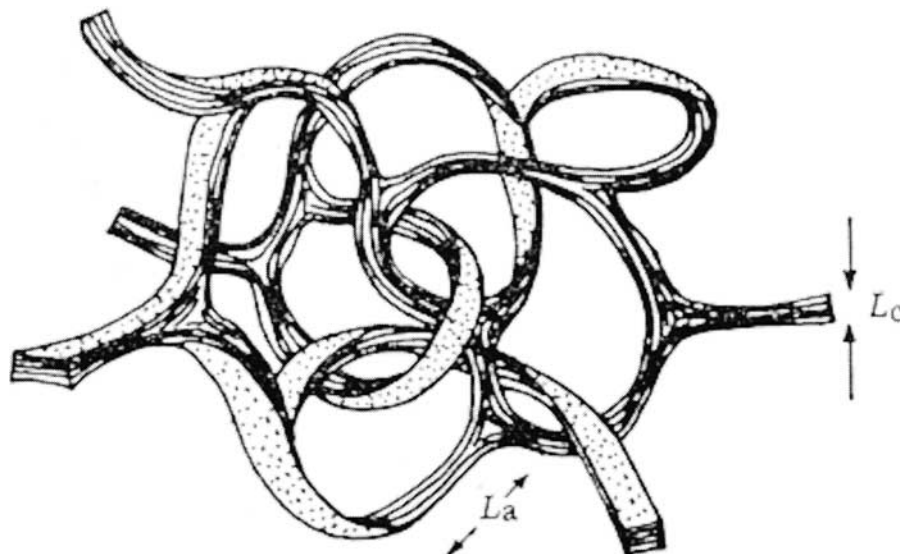


FIG. 15. The Jenkins-Kawamura model of glassy carbon.<sup>32,58,59</sup>

microstructures and mechanical properties of carbon fibers derived from the two precursors vary considerably. This results from the fact that PAN is a non-graphitizing carbon whereas pitch is graphitizing. Thus, PAN-derived fibers only contain very small graphitic domains, and have a large number of voids, giving them a relatively low density. This lack of extended structure makes ex-PAN fibers relatively insensitive to flaws, giving them exceptionally high strengths. Because pitch is a graphitizing carbon, pitch-derived fibers have a much more perfect graphitic structure, which gives them a higher density and results in higher elastic moduli than for the PAN fibers.

X-ray diffraction of PAN-derived fibers produces crystallite lengths in the  $a$  direction of approximately 4–10 nm depending on the annealing temperature.<sup>68</sup> High-resolution TEM shows that the fibers have an imperfect structure, containing many elongated voids. Several models have been put forward for the structure of PAN-derived carbon fibers, all based on the assumption that the basic structural units are graphite sheets or ribbons. A model suggested by Crawford and Johnson<sup>1</sup> is shown in Figure 1(a). Here, the structure consists of a random arrangement of flat or crumpled graphite sheets, with all the  $a$ - $b$  planes running parallel to the fiber axis. However, given the flexibility

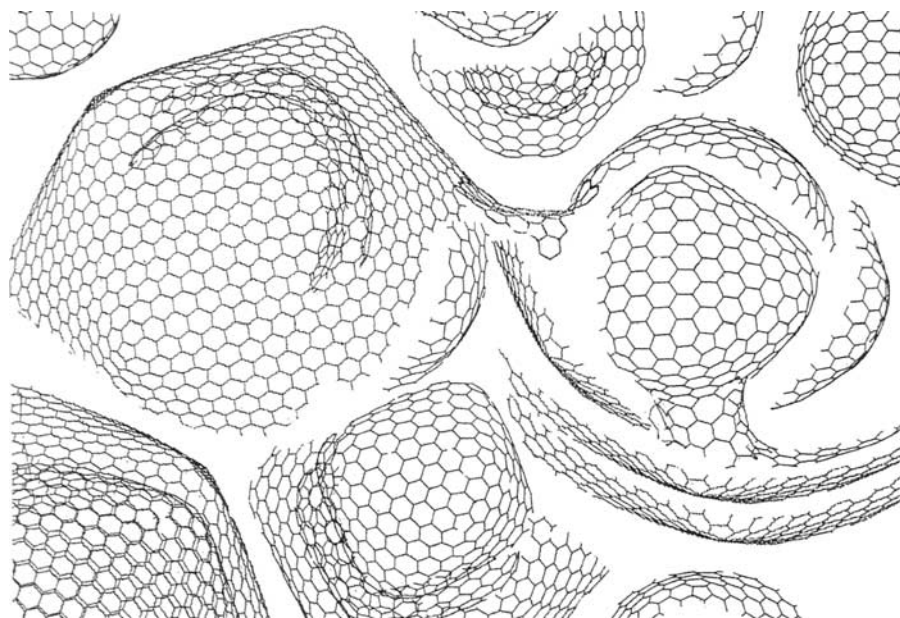


FIG. 16. Model for the structure of high temperature glassy carbon containing fullerene-like elements.<sup>60</sup>

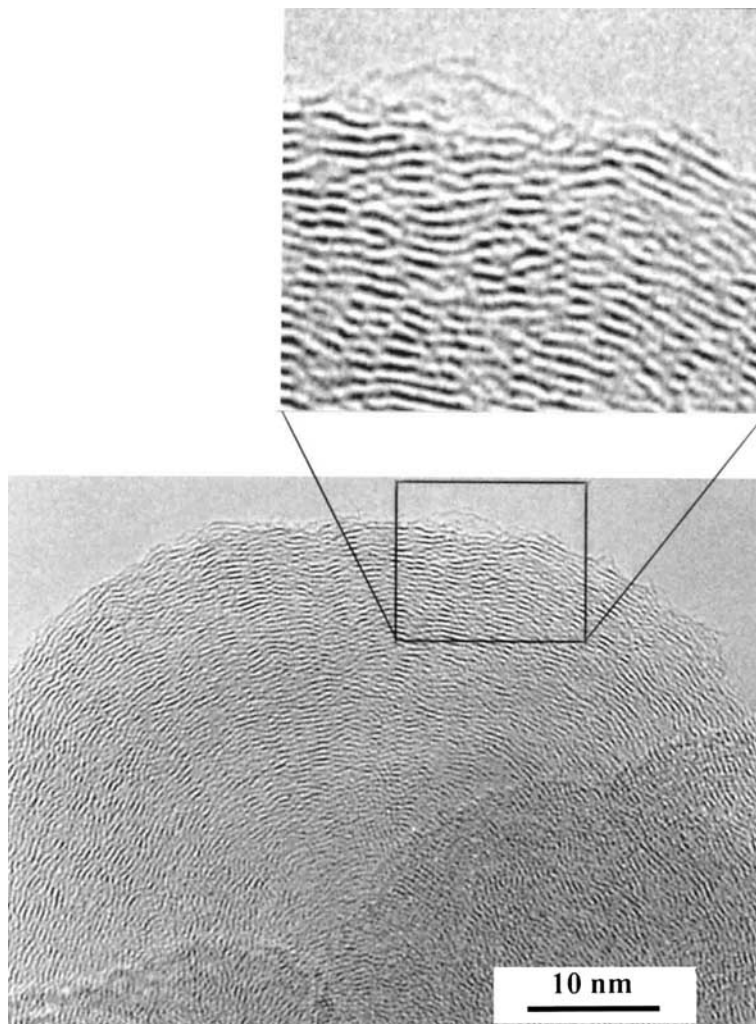


FIG. 17. HRTEM image of commercial carbon black particle. Enlarged area shows individual graphene layers.

of graphite sheets, it is difficult to see how the voids in such a structure could survive high-temperature heat treatment. Therefore, the possibility that the voids in fact result from the presence of fullerene-like elements is worthy of consideration. The elongated shapes of the voids suggests that they may have structures related to those of carbon nanotubes, but further HRTEM studies will be needed to confirm this possibility.

## CARBON BLACK

### Background

Carbon black, which is essentially a pure form of soot, is manufactured industrially on a large scale, primarily for use as a filler in rubber products. It is also used as a pigment and as a component of xerographic toners.<sup>71</sup> A variety of industrial processes are used, the most important of which is the “furnace black” process, which involves the partial combustion of petrochemical or coal tar oils. Carbon black consists of quasi-spherical particles ranging from about 10 nm to about 500 nm

in size, which are often joined together in clusters or “necklace” chains. A transmission electron micrograph of a typical carbon black particle is shown in Figure 17. Before discussing the evidence for fullerene-like structures in carbon black, a very brief summary will be given of the basic aspects of carbon black formation as they are currently understood. More detail can be found in Refs. 71–74.

It is believed that carbon black particles form in three distinct phases. The first stage, known as particle inception, involves homogeneous reactions between hydrocarbon species that combine into larger aromatic layers and eventually condense out of the vapor phase to form nuclei. In the second stage, called growth, two processes occur: nuclei coalescence and surface deposition, the latter process being responsible for most of the mass increase of the primary particles. Finally, in the chain formation stage, relatively large spheroidal particles become joined together, without coalescing, to form long chains. Many aspects of this mechanism are poorly understood, in particular the nature of the initial nucleus.

### Structure of Carbon Black Particles

The first X-ray diffraction studies of carbon black and soot particles were carried out by Warren in the 1930s and 1940s,<sup>75,76</sup> who demonstrated the presence of layer planes of graphite-like carbon. However, no evidence of the three-dimensional graphite structure was detected. Many subsequent X-ray diffraction studies have been carried out,<sup>74</sup> enabling the dimensions of the individual crystallites to be determined. The two parameters used to characterize the structure of disordered carbons are  $L_a$ , the length of the fragment in the in-plane direction and  $L_c$  the length in the  $c$  direction. For carbon blacks,  $L_a$  usually falls in the range 1–3 nm, whereas  $L_c$  is usually of the order of 1.5 nm. However, these values probably underestimate the size of the sheets that make up carbon black, as discussed later.

X-ray diffraction reveals the nature of the basic structural units, but detailed information on the internal organization of the carbon black particles can only be achieved through high-resolution electron microscopy. A review of early TEM studies of carbon black was given by Heidenreich, Hess, and Ban in 1968.<sup>77</sup> These authors interpreted the TEM results in terms of the model shown in Figure 18. In this model, the basic structural units are rather flat graphene planes, arranged in a concentric manner around a hollow center. However, more recent high-resolution TEM studies of carbon black particles show that the structural units making up the particles are less perfect, and also somewhat larger than those envisaged by Heidenreich *et al.* (see Figure 17).

Following their discovery of  $C_{60}$  in 1985, Kroto, Smalley, and their co-workers became interested in the subject of soot and carbon black formation. In 1986 they put forward a new mechanism for soot formation, the icospiral growth mechanism,<sup>78</sup> which was later refined by Kroto and McKay.<sup>15</sup> The mechanism was based on the “pentagon-road” model of fullerene formation.<sup>79</sup> The essential element of the pentagon-road model is the incorporation

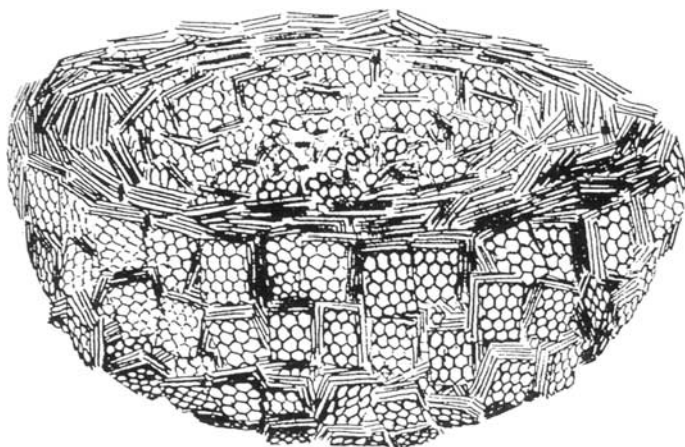


FIG. 18. The Heidenreich-Hess-Ban model of carbon black structure.<sup>77</sup>

of pentagonal rings into a growing carbon network, driven by the need to eliminate dangling bonds. If the pentagons occur in the “correct” positions then  $C_{60}$  and other fullerenes will result, but in general closed structures will not be formed. Kroto and Smalley suggested that if the growing shell fails to close, it would tend to curl around on itself like a nautilus shell. In the refined model,<sup>15</sup> Kroto and McKay suggested that the pentagons in a new layer would tend to form directly above those in the previous layer in an epitaxial manner, resulting in twelve columns of pentagonal rings. They argued that the spiralling structure would become increasingly faceted as it grew larger, in the same way that giant fullerenes are expected to be much more faceted than small ones.

It would be fair to say that the ideas of Kroto *et al.* on the growth of soot and carbon black particles were not received favorably by experts in the field. In particular Frenklach and Ebert have argued strongly against the idea that fullerenes have any relevance to soot formation. They based their arguments, among other things, on evidence from  $^{13}C$  NMR spectroscopy of soot.<sup>80,81</sup> They pointed out that  $^{13}C$  NMR spectra of soot resemble those of aromatic molecules much more closely than those of fullerenes. These authors have also stated that the kinetics of soot formation are inconsistent with the icospiral model of the structure. They have used computer simulations to show that the growth of shell structures would be much slower than those of planar fragments. Soot formation is known to be extremely rapid, so it seemed unlikely that shell growth of the kind described by Kroto and colleagues could be involved.

High-resolution TEM studies have also cast doubt on the models put forward by Kroto and colleagues. The Kroto–McKay model implies that carbon black particles should have rather perfect structures, perhaps resembling the “carbon onions” first observed by Ugarte.<sup>82</sup> However, as already noted, high-resolution TEM images reveal rather disordered structures. It can be seen from the enlarged region in Figure 17 that the individual graphene layers that make up structure are not flat, but rather wavy and curved. Importantly, the layers are not preferentially curved about the center of the particle, as might be expected if the “icospiral” model were correct. Detailed analyses of HRTEM images of carbon black particles have been carried out by several groups.<sup>12,83–85</sup> Palotás and colleagues used filtering techniques to remove noise from the images and reveal clearly the contrast from individual carbon planes.<sup>83</sup> An example of their filtered images is reproduced in Figure 19. This again shows the planes to be wrinkled rather than flat, and that there is no preferential curvature about the center. Vander Wal and colleagues have reported similar results.<sup>84</sup> It appears likely that the curvature observed in the individual carbon planes is due to the presence of non-hexagonal rings, but that these fullerene structures do not explain the sphericity of the carbon black particles. Instead, the roundness of the particles is believed to be a consequence of energetics, coupled with surface mass growth via a radical addition mechanism.<sup>72,73</sup>



FIG. 19. Filtered pattern of soot particle structure.<sup>83</sup>

### Effect of High-Temperature Heat Treatment on Carbon Black Structure

As discussed in “evidence for fullerene-like structures in microporous carbons” the effect of high temperature heat treatments on carbon materials may provide clues to the structure of the original carbons. It is well established that such treatments transform carbon black particles into faceted particles that sometimes appear to have closed shell-like structures. The precise structure of the graphitized particles depends on the nature of the original carbon black. In some cases, relatively large, discrete particles are formed,<sup>86</sup> while other graphitized carbon blacks have a less well-defined structure, with many bent and faceted layer planes and some apparently closed shell structures.<sup>87,88</sup> The presence of faceted planes and closed structures in the heat-treated carbon is indicative of the presence of pentagonal rings, and suggests that fullerene-like elements may have been present in the original particles. On the other hand, it is possible that the pentagons may have formed during the heat treatment. Further detailed TEM work might help to clarify this.

### CONCLUSIONS

Until quite recently, the structure of microporous carbons and other  $sp^2$ -bonded carbons has been discussed in terms of models based on “flat graphite.” This article has set out to review the evidence that such carbons might have fullerene-related structures. The article began with a detailed discussion of the structure of non-graphitizing carbons. The idea that these carbons may be fullerene-like in structure would help to explain many of their characteristics, including their low density, microporosity, and hardness. There would also be implications for understanding

their adsorptive properties. A large volume of theoretical work has been carried out on gas adsorption in carbons,<sup>89–92</sup> prompted by their enormous commercial importance. In many cases these theoretical discussions have utilized structural models based on “flat carbon.” For example, Thomson and Gubbins used reverse Monte Carlo techniques to generate model carbon structures composed of “plates” in which all the atoms are in hexagonal rings.<sup>90</sup> Many theoretical treatments have assumed that the carbon pores have a slitlike shape, confined by parallel planes.<sup>92</sup> If the fullerene-like models are correct, these ideas may have to be modified, and there have already been a few theoretical studies of adsorption on fullerene-related carbons.<sup>93,94</sup>

Fullerene-like models may also help in understanding the “activation” process that is essential for developing a very high surface area in non-graphitizing carbons. Activation usually involves treatment with a mild oxidizing agent, such as  $CO_2$  or water vapor, and it is generally believed that this has the effect of burning away carbon fragments inside micropores, thus enhancing surface area.<sup>27</sup> However, if the new models for the structure of microporous carbons are correct, then this activation treatment may also have a further consequence. It is known that mild oxidation, for example with  $CO_2$  at  $850^\circ C$ , can remove the caps from carbon nanotubes by selectively attacking the pentagonal carbon rings.<sup>95</sup> If microporous carbons have a fullerene-like structure, then the effect of such a treatment would be to open closed pores by selective attack of the pentagons, thus significantly increasing the surface area.

It is important to stress that there is as yet no *direct* proof that non-graphitizing carbons contain pentagonal rings. Methods such as X-ray and neutron diffraction do not provide unequivocal evidence that pentagons or other non-hexagonal rings are present. However, it is possible that direct imaging of pentagonal rings may be possible using transmission electron microscopy. In recent work, Iijima and colleagues have obtained atomic resolution images of defects in graphene layers using HRTEM.<sup>96,97</sup> Their method involved reconstructing the images from Fourier transforms of the TEM images. Imaging of pentagons might be possible using this method, or alternatively by using the new aberration-corrected TEMs<sup>98</sup> and STEMs.<sup>99</sup> Initial studies of carbon nanotubes using these methods have produced promising results.<sup>100</sup>

Glassy carbon and PAN-derived carbon fibers have also been discussed. In the case of glassy carbon, high-resolution TEM again supplies evidence for a fullerene-related structure. New models for glassy carbon that incorporate non-hexagonal rings<sup>60</sup> seem to provide a better basis for understanding their properties than older models such as that of Jenkins and Kawamura.<sup>32</sup> There also seem to be good reasons for believing that PAN-derived carbon fibers and other high-strength carbon fibers may be fullerene-related, and further studies of these materials using HRTEM and other techniques would be valuable.

Concerning carbon black particles, it appears that the long-standing problem of their detailed structure remains unresolved. A number of points can be made with reasonable confidence,

however. The venerable, and much reproduced, model put forward by Heidenreich *et al.* (Figure 18) seems to be overly simplistic. Although it is true that the basic structural units that make up the particles are arranged concentrically around the center, HRTEM images suggest that the units are more extensive, and more defective, than the rather perfect fragments in the Heidenreich model. There also seems to be little evidence to support the icospiral growth model of Kroto, Smalley *et al.* This model predicts that carbon black particles should have a relatively ordered structure, rather than the disordered structure that is observed experimentally. Detailed TEM studies show that fullerene-like structures are probably present, but are not responsible for the sphericity of the particles. This is another area where ultra-high resolution TEM would be of great value.

### ACKNOWLEDGMENTS

The author is grateful to Randy Vander Wal for helpful comments.

### REFERENCES

1. D. Crawford and D. J. Johnson, High-resolution electron microscopy of high-modulus carbon fibres, *J. Microscopy* **94**, 51 (1971).
2. L. L. Ban, D. Crawford, and H. Marsh, Lattice-resolution electron-microscopy in structural studies of non-graphitizing carbons from polyvinylidene chloride (PVDC), *J. Appl. Cryst.* **8**, 415 (1975).
3. H. W. Kroto, J. R. Heath, S. C. O'Brien, R. F. Curl, and R. E. Smalley, C<sub>60</sub>: Buckminsterfullerene, *Nature* **318**, 162 (1985).
4. W. Krätschmer, L. D. Lamb, K. Fostiropoulos, and D. R. Huffman, Solid C<sub>60</sub>: a new form of carbon, *Nature* **347**, 354 (1990).
5. H. W. Kroto, C<sub>60</sub>: Buckminsterfullerene, the celestial sphere that fell to earth, *Angewandte Chemie* **31**, 111 (1992).
6. S. Iijima, Helical microtubules of graphitic carbon, *Nature* **354**, 56 (1991).
7. P. J. F. Harris, *Carbon Nanotubes and Related Structures*. Cambridge University Press 1999.
8. O. A. Shenderova, V. V. Zhirnov, and D. W. Brenner, Carbon nanostructures, *Crit. Rev. Solid State Mater. Sci.* **27**, 227 (2002).
9. P. J. F. Harris, S. C. Tsang, J. B. Claridge, and M. L. H. Green, high-resolution electron microscopy studies of a microporous carbon produced by arc-evaporation, *J. Chem. Soc., Faraday Trans.* **90**, 2799 (1994).
10. S. Iijima, M. Yudasaka, R. Yamada, S. Bandow, K. Suenaga, F. Kokai, and K. Takahashi, Nano-aggregates of single-walled graphitic carbon nano-horns, *Chem. Phys. Lett.* **309**, 165 (1999).
11. P. J. F. Harris, M. L. H. Green, and S. C. Tsang, High-resolution electron microscopy of tubule containing graphitic carbon, *J. Chem. Soc., Faraday Trans.* **89**, 1189 (1993).
12. W. J. Grieco, J. B. Howard, L. C. Rainey, and J. B. Vander Sande, Fullerenic carbon in combustion-generated soot, *Carbon*, **38**, 597 (2000).
13. F. Cataldo, The impact of a fullerene-like concept in carbon black science, *Carbon* **40**, 157 (2002).
14. P. J. F. Harris, Impact of the discovery of fullerenes on carbon science, *Chemistry and Physics of Carbon* **28**, 1 (2003).
15. H. W. Kroto and K. McKay, The formation of quasi-icosahedral spiral shell carbon particles, *Nature* **331**, 328 (1988).
16. P. W. Fowler and D. E. Manolopoulos, *An Atlas of Fullerenes*, Oxford University Press, Oxford, 1995.
17. E. Hernández, P. Ordejón, and H. Terrones, Fullerene growth and the role of nonclassical isomers, *Phys. Rev.* **B63**, 193403 (2001).
18. K. Fujine, T. Ishida, and J. Aihara, Localization energies for graphite and fullerenes, *Physical Chemistry—Chemical Physics* **3**, 3917 (2001).
19. I. Mochida, M. Egashira, Y. Korai, and K. Yokogawa, Structural changes of fullerene by heat-treatment up to graphitization temperature, *Carbon* **35**, 1707 (1997).
20. M. Ge and K. Sattler, Scanning tunneling microscopy of single-shell nanotubes of carbon, *Appl. Phys. Lett.* **65**, 2284 (1994).
21. S. Iijima, T. Ichihashi, and Y. Ando, Pentagons, heptagons and negative curvature in graphitic microtubule growth, *Nature* **356**, 776 (1992).
22. Y. Ando and S. Iijima, Preparation of carbon nanotubes by arc-discharge evaporation, *Jpn. J. Appl. Phys.* **32**, L107 (1993).
23. S. Iijima and T. Ichihashi, Single-shell carbon nanotubes of 1-nm diameter, *Nature* **363**, 603 (1993).
24. D. S. Bethune, C. H. Kiang, M. S. de Vries, G. Gorman, R. Savoy, J. Vasquez, and R. Beyers, Cobalt-catalysed growth of carbon nanotubes with single-atomic-layer walls, *Nature* **363**, 605 (1993).
25. R. E. Franklin, Crystallite growth in graphitizing and non-graphitizing carbons, *Proc. Roy. Soc.* **A209**, 196 (1951).
26. P. J. F. Harris, Rosalind Franklin's work on coal, carbon, and graphite, *Interdisciplinary Science Reviews* **26**, 204 (2001).
27. H. Jankowska, A. Swiatkowski, and J. Choma, *Active Carbon*, Ellis Horwood, New York, 1991.
28. J. W. Patrick (ed.), *Porosity in Carbons: Characterisation and Applications*, Arnold, London, 1994.
29. R. C. Bansal and M. Goyal, *Activated Carbon Adsorption*. Taylor & Francis, London, 2005.
30. P. J. F. Harris, A. Burian, and S. Duber, High-resolution electron microscopy of a microporous carbon, *Phil. Mag. Lett.* **80**, 381 (2000).
31. J. J. Kipling, J. N. Sherwood, P. V. Shooter, and N. R. Thompson, The pore structure and surface area of high-temperature polymer carbons, *Carbon* **1**, 321 (1964).
32. G. M. Jenkins and K. Kawamura, Structure of glassy carbon, *Nature* **231**, 175 (1971).
33. D. Ugarte, Morphology and structure of graphitic soot particles generated in arc-discharge C<sub>60</sub> production, *Chem. Phys. Lett.* **198**, 596 (1992).
34. A. Oberlin, Application of dark-field electron-microscopy to carbon study, *Carbon* **17**, 7 (1979).
35. A. Oberlin, High-resolution TEM studies of carbonization and graphitization, *Chemistry and Physics of Carbon* **22**, 1 (1989).
36. S. Ergun and V. H. Tiensuu, Tetrahedral structures in amorphous carbons, *Acta Cryst.* **12**, 1050 (1959).
37. S. Ergun and L. E. Alexander, Crystalline forms of carbon: A possible hexagonal polymorph of diamond, *Nature* **195**, 765 (1962).
38. P. J. F. Harris and S. C. Tsang, High-resolution electron microscopy studies of non-graphitizing carbons, *Phil. Mag.* **A76**, 667 (1997).

39. P. J. F. Harris, Structure of non-graphitising carbons, *International Materials Reviews* **42**, 206 (1997).
40. A. Burian, A. Ratuszna, J. C. Dore, and S. W. Howells, Radial distribution function analysis of the structure of activated carbons, *Carbon* **36**, 1613 (1998).
41. J. C. Dore, M. Sliwinski, A. Burian, S. W. Howells, and D. Cazorla, Structural studies of activated carbons by pulsed neutron diffraction, *Journal of Physics—Condensed Matter* **11**, 9189 (1999).
42. V. Petkov, R. G. DiFrancesco, S. J. L. Billinge, M. Acharya, and H. C. Foley, Local structure of nanoporous carbons, *Phil. Mag.* **B79**, 1519 (1999).
43. P. Zetterstrom, S. Urbonaite, F. Lindberg, R. G. Delaplane, J. Leis, and G. Svensson, Reverse Monte Carlo studies of nanoporous carbon from TiC, *Journal of Physics—Condensed Matter* **17**, 3509 (2005).
44. M. A. Smith, H. C. Foley, and R. F. Lobo, A simple model describes the PDF of a non-graphitizing carbon, *Carbon* **42**, 2041 (2004).
45. P. H. Tan, S. Dimovski, and Y. Gogotsi, Raman scattering of non-planar graphite: Arched edges, polyhedral crystals, whiskers and cones, *Phil. Trans. Roy. Soc.* **A362**, 2289 (2004).
46. A. Burian and J. C. Dore, Does carbon prefer flat or curved surfaces?, *Acta Physica Polonica* **A98**, 457 (2000).
47. S. J. Townsend, T. J. Lenosky, D. A. Muller, C. S. Nichols, and V. Elser, Negatively curved graphitic sheet model of amorphous-carbon, *Phys. Rev. Lett.* **69**, 921 (1992).
48. S. C. Tsang, P. J. F. Harris, J. B. Claridge, and M. L. H. Green, A microporous carbon produced by arc-evaporation, *J. Chem. Soc., Chem. Comm.* 1519 (1993).
49. L. A. Bursill and L. N. Bourgeois, Image-analysis of a negatively curved graphitic sheet model for amorphous-carbon, *Mod. Phys. Lett.* **B9**, 1461 (1995).
50. L. N. Bourgeois and L. A. Bursill, High-resolution transmission electron microscopy study of a cross-linked fullerene-related multilayer graphitic material, *Phil. Mag.* **A79**, 1155 (1999).
51. W. A. de Heer and D. Ugarte, Carbon onions produced by heat-treatment of carbon soot and their relation to the 217.5 nm interstellar absorption feature, *Chem. Phys. Lett.* **207**, 480 (1993).
52. D. Ugarte, High-temperature behaviour of “fullerene black,” *Carbon* **32**, 1245 (1994).
53. I. C. Lewis, Chemistry of carbonization, *Carbon* **20**, 519 (1982).
54. A. V. Gribanov and Y. N. Sazanov, Carbonization of polymers, *Russian Journal of Applied Chemistry* **70**, 839 (1997).
55. A. Kumar, R. F. Lobo, and N. J. Wagner, Porous amorphous carbon models from periodic Gaussian chains of amorphous polymers, *Carbon* **43**, 3099 (2005).
56. M. Acharya, M. S. Strano, J. P. Mathews, J. L. Billinge, V. Petkov, S. Subramoney, and H.C. Foley, Simulation of nanoporous carbons: A chemically constrained structure, *Phil. Mag.* **B79**, 1499 (1999).
57. K. Kinoshita, *Carbon: Electrochemical and Physicochemical Properties*, Wiley, New York, 1988.
58. G. M. Jenkins, K. Kawamura and L. L. Ban, Formation and structure of polymeric carbons, *Proc. Roy. Soc.* **A327**, 501 (1972).
59. G. M. Jenkins and K. Kawamura, *Polymeric carbons—Carbon Fibre, Glass and Char*, Cambridge University Press, 1976.
60. P. J. F. Harris, Fullerene-related structure of commercial glassy carbons, *Phil. Mag.* **A84**, 3159 (2004).
61. J. Kakinoki, A model for the structure of “glassy carbon,” *Acta Cryst.* **18**, 578 (1965).
62. D. F. R. Mildner and J. M. Carpenter, On the short-range atomic-structure of non-crystalline carbon, *J. Non-cryst. Solids* **47**, 391 (1982).
63. L. A. Pesin, Structure and properties of glass-like carbon, *J. Mater. Sci.* **37**, 1 (2002).
64. L. A. Pesin and E. M. Baitinger, A new structural model of glass-like carbon, *Carbon* **40**, 295 (2002).
65. Y. Gogotsi, J. A. Libera, N. Kalashnikov, and M. Yoshimura, Graphite polyhedral crystals, *Science* **290**, 317 (2000).
66. P. Morgan, *Practical Guide to Carbon Fibers and Their Composites*, CRC Press, Boca Raton, 2004.
67. M. S. Dresselhaus, G. Dresselhaus, K. Sugihara, I. L. Spain, and H. A. Goldberg, *Graphite Fibers and Filaments*, Springer-Verlag, Berlin, 1988.
68. D. J. Johnson, Recent advances in studies of carbon-fiber structure, *Phil. Trans. Roy. Soc.* **A294**, 443 (1980).
69. W. N. Reynolds, Structure and properties of carbon fibers, *Chemistry and Physics of Carbon* **11**, 1 (1973).
70. L. H. Peebles, Carbon fibres—structure and mechanical-properties, *International Materials Reviews* **39**, 75 (1994).
71. J.-B. Donnet, R. C. Bansal, and M.-J. Wang, *Carbon black*, 2nd ed., Marcel Dekker, New York, 1993.
72. H. P. Palmer and C. F. Cullis, The formation of carbon from gases, *Chemistry and Physics of Carbon* **1**, 265 (1965).
73. S. J. Harris and A. M. Weiner, Chemical kinetics of soot particle growth, *Ann. Rev. Phys. Chem.* **36**, 31 (1985).
74. J.-B. Donnet, 50 years of research and progress on carbon-black, *Carbon* **32**, 1305 (1994).
75. B. E. Warren, X-ray diffraction study of carbon black, *J. Chem. Phys.* **2**, 551 (1934).
76. B. E. Warren, X-ray diffraction in random layer lattices, *Phys. Rev.* **59**, 693 (1941).
77. R. D. Heidenreich, W. M. Hess, and L. L. Ban, A test object and criteria for high resolution electron microscopy, *J. Appl. Cryst.* **1**, 1 (1968).
78. Q. L. Zhang, S. C. O’Brien, J. R. Heath, Y. Liu, R. F. Curl, H. W. Kroto, and R. E. Smalley, Reactivity of large carbon clusters: Spheroidal carbon shells and their possible relevance to the formation and morphology of soot, *J. Phys. Chem.* **90**, 525 (1986).
79. J. R. Heath, S. C. O’Brien, R. F. Curl, H. W. Kroto, and R. E. Smalley, Carbon condensation, *Comments Cond. Mat. Phys.* **13**, 119 (1987).
80. M. Frenklach and L. B. Ebert, Comment on the proposed role of spheroidal carbon clusters in soot formation, *J. Phys. Chem.* **92**, 561 (1988).
81. L. B. Ebert, The interrelationship of C<sub>60</sub>, soot and combustion, *Carbon* **31**, 999 (1993).
82. D. Ugarte, Curling and closure of graphitic networks under electron-beam irradiation, *Nature* **359**, 707 (1992).
83. A. B. Palotás, L. C. Rainey, C. J. Feldermann, A. F. Sarofim, and J. B. Vander Sande, Soot morphology: An application of image

- analysis by high-resolution transmission electron microscopy, *Micros. Res. Tech.* **33**, 266 (1996).
84. R. L. Vander Wal, A. J. Tomasek, M. I. Pamphlet, C. D. Taylor, and W. K. Thompson, Analysis of HRTEM images for carbon nanostructure quantification, *J. Nanoparticle Research* **6**, 555 (2004).
  85. A. Goel, P. Hebgren, J. B. Vander Sande, and J.B. Howard, Combustion synthesis of fullerenes and fullerene nanostructures, *Carbon* **40** 177 (2002).
  86. D. Graham and W. S. Kay, The morphology of thermally graphitized P-33 carbon black in relation to absorbent uniformity, *J. Colloid Sci.* **16**, 182 (1961).
  87. P. A. Marsh, A. Voet, T. J. Mullins, and L. D. Price, Quantitative micrography of carbon black microstructure, *Carbon* **9**, 797 (1971).
  88. R. L. Vander Wal, A. J. Tomasek, K. Street, D. R. Hull, and W. K. Thompson, Carbon nanostructure examined by lattice fringe analysis of high-resolution transmission electron microscopy images, *Applied Spectroscopy* **58**, 230 (2004).
  89. M. B. Sweatman and N. Quirke, "Modelling gas adsorption in amorphous nanoporous materials," in *The Handbook of Theoretical and Computational Nanotechnology*, edited by M. Rieth and W. Schommers, American Scientific Publishers, Stevenson Ranch, 2005.
  90. K. T. Thomson and K. E. Gubbins, Modeling structural morphology of microporous carbons by reverse Monte Carlo, *Langmuir* **16**, 5761 (2000).
  91. T. J. Bandosz, M. J. Biggs, K. E. Gubbins, Y. Hattori, T. Iiyama, K. Kaneko, J. Pikunic, and K. T. Thomson, Molecular models of porous carbons, *Chemistry and Physics of Carbon* **28**, 41 (2003).
  92. M. B. Sweatman and N. Quirke, Modelling gas adsorption in slit-pores using Monte Carlo simulation, *Molecular Simulation* **27**, 295 (2001).
  93. J. W. Jiang, J. B. Klauda, and S. I. Sandler, Monte Carlo simulation of O<sub>2</sub> and N<sub>2</sub> adsorption in nanoporous carbon (C<sub>168</sub> schwarzite), *Langmuir* **19**, 3512 (2003).
  94. J. W. Jiang, N. J. Wagner, and S. I. Sandler, A Monte Carlo simulation study of the effect of carbon topology on nitrogen adsorption on graphite, a nanotube bundle, C<sub>60</sub> fullerite, C<sub>168</sub> schwarzite, and a nanoporous carbon, *Physical Chemistry—Chemical Physics* **6**, 4440 (2004).
  95. S. C. Tsang, P. J. F. Harris, and M. L. H. Green, Thinning and opening of carbon nanotubes by oxidation using carbon dioxide, *Nature* **362**, 520 (1993).
  96. A. Hashimoto, K. Suenaga, A. Gloter, K. Urita, and S. Iijima, Direct evidence for atomic defects in graphene layers, *Nature* **430**, 870 (2004).
  97. H. Zhu, K. Suenaga, A. Hashimoto, K. Urita, and S. Iijima, Structural identification of single and double-walled carbon nanotubes by high-resolution transmission electron microscopy, *Chem. Phys. Lett.* **412**, 116 (2005).
  98. M. Haider, H. Uhlemann, E. Schwan, H. Rose, B. Kabius, and K. Urban, Electron microscopy image enhanced, *Nature* **392**, 768 (1998).
  99. P. E. Batson, N. Dellby, and O. L. Krivanek, Sub-Ångstrom resolution using aberration corrected electron optics, *Nature* **418**, 617 (2002).
  100. N. Tanaka, J. Yamasaki, T. Kawai, and H. Pan, The first observation of carbon nanotubes by spherical aberration corrected high-resolution transmission electron microscopy, *Nanotechnology* **15**, 1779 (2004).